

## Molecular Dynamics Simulations of Osmosis and Reverse Osmosis in Solutions

S. MURAD

*Chemical Engineering Department, University of Illinois at Chicago, Chicago IL 60607, USA*

**Abstract.** Computer simulation studies using the method of molecular dynamics have been carried out to investigate osmosis and reverse osmosis in solutions separated by semi-permeable membranes. The method has been used to study the dynamic approach to equilibrium in such systems from their initial nonequilibrium state. In addition density profiles of both the solute and solvent molecules have been investigated, especially near the walls for adsorption effects. Finally the diffusion coefficients and osmotic pressure have also been measured.

Our results show both osmosis and reverse osmosis, as well as a smooth transition between the two when either the solution concentration is changed, or the density (pressure) difference between the solvent and solution compartments is varied. We believe this new method can be used to improve our understanding of these two important phenomena at the molecular level.

**Keywords:** osmosis, reverse osmosis, adsorption, diffusion, molecular dynamics

### 1. Introduction

The phenomena of osmosis and reverse osmosis are of considerable importance in both the life and physical sciences, and takes place in both liquids and gases. Reverse osmosis is also a rather energy efficient method for separations, and has shown considerable promise in processes as diverse as desalination, waste-treatment, as well as food processing (e.g., concentrating orange juice without affecting its taste) (Hoornaert, 1984; Sourirajan, 1970). In this paper we report results of computer simulations to study osmosis and reverse osmosis in solutions. The computer simulations have been carried out using a new method developed by us to study fluids confined by semi-permeable membranes, based on microcanonical (NVE) molecular dynamics. (Murad et al., 1993; 1993a). A unique feature of our method is that it allows for a gradual transition from impermeable to semi-permeable to totally permeable walls, while maintaining the atomic nature of the confining wall. Although atomically rough walls have been studied by others as well (Banavar et al., 1990; Mo and Rosenberger, 1990; Bojan et al., 1992) the

methods used do not allow for the permeability of the walls to the confined fluids to be controlled as easily. In the studies reported here the walls have been designed to be permeable to the solvent molecules while completely impermeable to the solute molecules. The dynamic approach to equilibrium from the initial conditions has been carefully monitored in these simulations. The properties investigated include the net movement of solvent molecules across the semi-permeable walls, the rate of diffusion of the solute and solvent molecules, the density profiles (especially near the walls for adsorption effects) as well as the osmotic pressure. Our results show a rather interesting transition from osmosis to reverse osmosis, as the pressure difference across the membrane, or the concentration of the solution is varied.

Osmosis and reverse osmosis are generally carried out experimentally at either constant volume (gases) or constant osmotic pressure (liquids) (Sourirajan, 1970). Since the natural molecular dynamics ensemble is microcanonical, we have used it in our work. This leads to a constant volume simulation. At equilibrium, all ensembles should lead to equivalent results.

## 2. The Model

In the method used, the atoms that constitute the membrane walls, are tethered to their equilibrium positions by a simple harmonic potential (Murad et al., 1993), as is the case in experiments, where the actual membrane is tethered to a suitable porous support. The structure of a typical wall so formed is given in Fig. 1. One setup of our simulation system is given in Fig. 2 in which  $L_x = L_y = L_z$ . A second setup was also investigated in which  $L_x = 2L_y = 2L_z$  and consequently the distance between the two semi-permeable membranes was twice that shown in Fig. 2. This allowed us to study the wall effects more precisely, because fewer molecules, as a fraction of the total molecules, were now nearest neighbors of the molecules that constitute the wall. The dotted line indicates the simulation system that is replicated in all three directions using the usual periodic boundary conditions. The simulation cube contained up to 256 (or 512 in the second setup) particles, of which 64 constituted the two semi-permeable walls. The solution compartment initially contains  $96 - N_B$  (or  $224 - N_B$ ) solvent particles, and  $N_B$  solute particles, while the solvent compartment initially contains  $N_S$  solvent molecules, where  $N_S$  varies

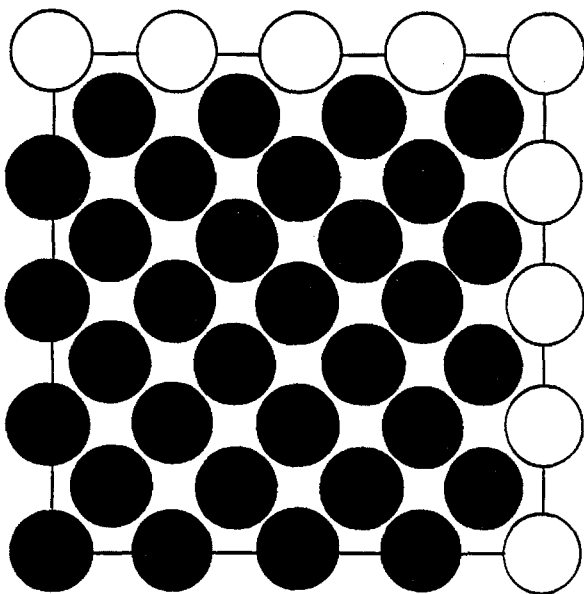


Figure 1. A typical structure, approximately to scale, of the membrane wall formed by tethering. The open circles are particles resulting from periodic boundary conditions. The intermolecular parameters of the wall particles as well as the spring constant for tethering can be used to vary the permeability of the wall.

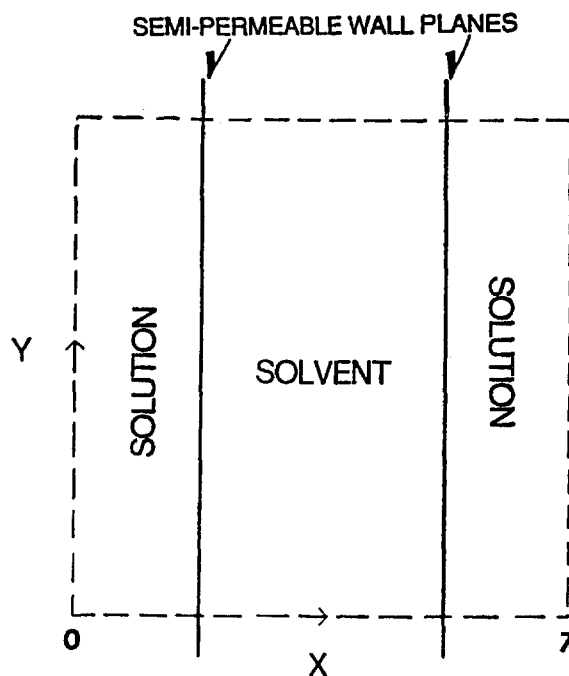


Figure 2. The  $xy$  projection of the cubic simulation system. The semi-permeable walls are in the  $yz$  plane. Periodic boundary conditions automatically generate a pair of walls, infinite in the transverse direction, with alternating solutions and solvent compartments, each of thickness  $3.5\sigma$ . In the second simulation system this distance would be  $7\sigma$ .

between 0 and 96 (or 224). By varying the number of molecules in the solvent compartment, we can vary the initial conditions and in particular the initial pressure difference between the solution and the solvent compartments. As will be seen later, this can lead to either osmosis or reverse osmosis. All molecules interact with shifted force Lennard-Jones potential (LJsf3). All results will be reported in *reduced* units based on the *solute* LJ ( $\epsilon$  and  $\sigma$ ) parameters. The LJ diameters of the solvent and wall molecules in reduced units were 0.5 and 1.15 respectively. For cross interactions the Lorentz-Berthelot rules were used. The LJ energy parameters of the solute, solvent, and membrane were all equal. From our simulation we have confirmed that with a tethering spring constant of 200, the membrane wall is readily permeable to the solvent (although, as will be shown in the results as well, it obviously offers some resistance to the flow of the solvent molecules in the  $x$  direction), but completely impermeable to the solute. The size of the simulation system was fixed at 7 in the  $y$  and  $z$  directions, while in the  $x$  direction it was either 7 or 14, and equally divided between the

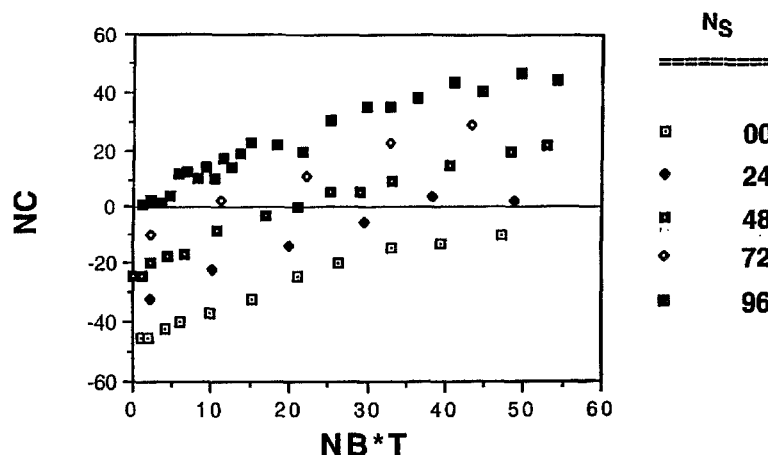


Figure 3. The net movement of solvent molecules ( $N_C$ ) from the solvent compartment to the solution compartment as the concentration of the solution varies, for the cubic system at different initial densities of the solvent ( $N_S$ ).

solvent and solution compartments. The simulations consisted of between 300,000 and 600,000 time steps of size 0.0025. This time step is smaller than usual for such systems, and was used so as to follow the vibrations of the tethered molecules accurately. The target temperature in our work was 1.075. In fact it was within  $\pm 0.075$  of this value. For the properties reported here, such variations in temperature are not expected to have any significant effect. At equilibrium the pressure difference across the wall, which is the osmotic pressure, was measured from the mean tether force on each wall necessary to keep the walls in place. The diffusion coefficients reported are based on the mean squared displacement of the solvent and solute particles. In the case of the solvent particles, which spend time in both the solution and solvent compartments, these are average values. The movement of the solvent molecules across the membrane was monitored. If the net movement of the solvent molecules is from the solvent to the solution compartment, osmosis results, while a net movement in the opposite direction would lead to reverse osmosis. As is perhaps obvious, reverse osmosis can be a useful method for separation of mixtures.

### 3. Results and Discussion

In our simulations the number of solute molecules in the solution compartment is varied between 0 and 100, while the number of solvent molecules in the solvent compartment, at the beginning of the simulation, varies between 0 and 224. When the number of molecules

in the solvent compartment is initially zero, clearly, only reverse osmosis can take place. At other initial values of the number of solvent molecules, both osmosis and reverse osmosis can be observed, depending upon the concentration of the solution. This can be seen clearly in Fig. 3 for the cubic simulation system ( $L = 7$ ). Similar results were also obtained for the second simulation system with  $L_x = 2L_y = 2L_z = 14$ .  $N_C$  represents the net movement of solvent molecules from the solvent to the solution compartment. Thus positive values of  $N_C$  represent osmosis, while negative values indicate reverse osmosis. Our results clearly show that the osmosis and reverse osmosis, are not two independent phenomena. They can both be seen in the same experiment, by simply changing the solution composition. This is illustrated in Fig. 3 for  $N_S = 48$  in particular. By changing the initial density of the solvent compartment we are changing the driving force for both osmosis and reverse osmosis, which depends on both this initial pressure difference between the solvent and solution compartment, as well as the osmotic pressure. The abscissa in these plots has been chosen to be  $N_B \cdot T$  ( $T$  varies by 3–4 per cent in these simulations), because it appears in the widely used van't Hoff's equation (van't Hoff, 1887; Taylor, 1925).

Another interesting result is the dynamic behavior of a system as it tries to come to a dynamic steady state condition, from its initial condition, either via osmosis or reverse osmosis. Figures 4(a) and 4(b) show such behavior for  $N_C$  for two typical systems, where at its initial state (a) the system is far, and (b) close to its final steady state (equilibrium) condition. In

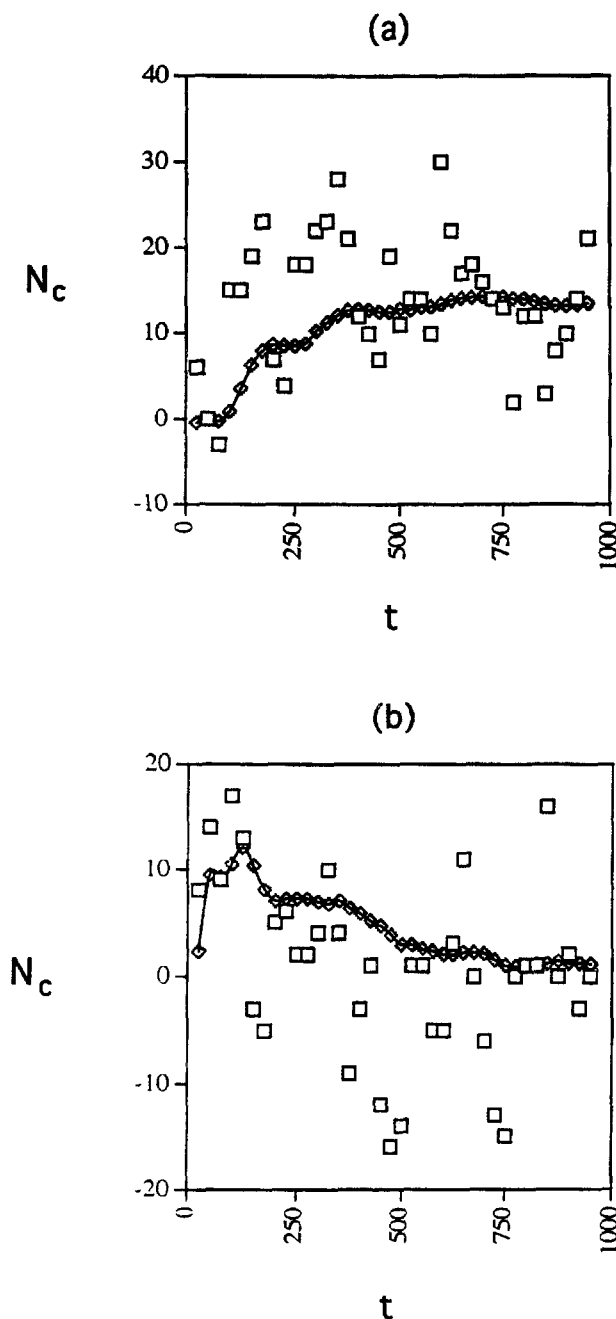


Figure 4. The dynamic approach to equilibrium, as observed by monitoring  $N_c$  when the initial conditions are (a) far from equilibrium; (b) close to equilibrium. ( $\square$ ) Instantaneous values, ( $\circ$ ) time averaged values.

both cases the final equilibrium condition is reached in about 200,000–300,000 time steps which corresponds to 500–750 units of time. Such equilibration has been found to take place faster in the smaller systems studied.

The results shown also include the instantaneous (not averaged) values of  $N_c$  in such systems. It is clear that even when, on a time averaged basis, the system has reached dynamic equilibrium, at any given instant, the density fluctuations in the solution and solvent compartments are still significant compared to the value of  $N_c$ . Such fluctuations in density are not in fact unusual even in homogeneous systems. If one were to divide a homogeneous 512 particle system, comparable to ours, into two equal volumes, it would not be unusual, for instance to find at any given instant 240 particles in one half rather than the average value of 256. We see such fluctuations in our system as well which are a result of the rapid and continuous exchange of the solvent molecules taking place between the two compartments. We would also like to point out that the instantaneous values have been shown only after every 10,000 steps, while the averaged values are averaged over *all* time steps. It is therefore not necessary (as appears to be the case here) for the average values to be the average of the instantaneous values shown in Fig. 4. Similar fluctuations were also noted in the osmotic pressure in such systems, as could have been expected.

The effective diffusion coefficients of the solute and solvent particles have been estimated from the mean squared displacements. In our case the diffusion tensor has two independent components,  $D_{\perp}$  defined as  $[\text{Lim}(t \rightarrow \infty) \langle x^2 \rangle / 2t]$ , and  $D_{\parallel}$  defined as  $[\langle (y^2 + z^2) \rangle / 4t]$ , where  $\langle \cdot \rangle$  is an average over the molecules. Since the wall is impermeable to the solute particles,  $D_{\perp}$  (w.r.t. the wall) of the solute particles is zero, as defined by us, and therefore only  $D_{\parallel}$  for the solute particles has been reported. Clearly near the center of the solution compartment the solute molecules do diffuse in the  $x$  direction. However, since the wall is impermeable to the solute particles, they keep bouncing back, leading to an effective value of zero for  $D_{\perp}$  of the solute molecules. At the center of the solution compartment, away from the walls, the system is almost homogeneous, so the actual values (not effective) of  $D_{\perp}$  and  $D_{\parallel}$  would be almost equal. We have previously found (Murad et al, 1993) that  $D_{\parallel}$  is insensitive to wall permeability. For the solvent molecules both  $D_{\perp}$  and  $D_{\parallel}$  can be calculated and have been reported. The solvent particles spend time in both the solution and solvent compartments (see Fig. 2), where their diffusion coefficients would presumably be different. The values reported for the solvent particle are averaged over the time spent in both these compartments. Figure 5 shows results for these three independent diffusion

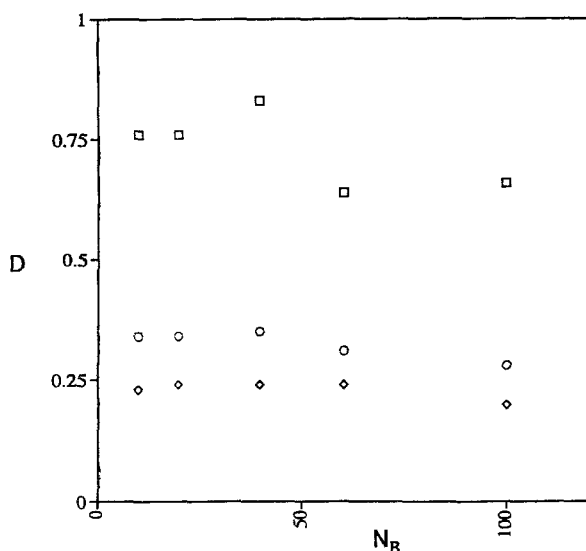


Figure 5. Diffusion coefficients of solute and solvent molecules in systems exhibiting both osmosis and reverse osmosis. ( $\circ$ )  $D_{\perp}$  solvent; ( $\square$ )  $D_{\parallel}$  solvent; ( $\diamond$ )  $D_{\parallel}$  solute.

coefficients for one typical set of simulations. They correspond to a system of size  $L_x = 2L_y = L_z = 14$ . Initially, the solution side consisted of  $N_B$  solute particles, and  $224 - N_B$  solvent particles. The solvent side initially had 112 solvent particles. At low solution concentrations this would lead to reverse osmosis while at higher concentrations to osmosis (see Fig. 3). The results reported show (and this was also found to be the case for other such sets studied) that the anisotropy of the solvent diffusion coefficient ( $D_{\perp}/D_{\parallel}$ ) is quite insensitive to the concentration of the solution (or indirectly the density as well, since the solute particles are much larger than the solvent particles). The anisotropy of the diffusion coefficient should depend primarily on the characteristics of the separating wall (although we have only studied one type of wall here). The individual diffusion coefficients do however decrease with an increase in the density (or solute concentration); the solute molecules being more sensitive to such changes, presumably because of their larger size in these studies. The size of the system itself, however does not seem to directly effect the diffusion coefficients significantly.

During the initial equilibration stage of the simulation, there is also diffusion across the membrane wall driven by the difference between the chemical potential of the solvent molecules in the solution and solvent compartments, which one may call osmotic diffusion. During this stage of the simulation the system is neither in an equilibrium state, nor steady state. It is therefore

not possible to calculate these osmotic diffusion coefficients, with an acceptable accuracy in the systems studied by us. The values reported are the self diffusion coefficients, obtained after equilibrium is reached.

The density profiles in the  $x$  direction for the solute and solvent for range of simulation parameters are shown in Figs. 6(a)–(d). Figure 6(a) corresponds to a cubic system of size  $L = 7$ , with  $N_B = 9$  and  $N_S = 96$ . Figure 6(b) corresponds to a system with  $L_x = 2L_y = 2L_z = 14$ ,  $N_B = 20$ , and  $N_S = 224$ . These two systems, thus, have approximately the same density and solute concentration. The only difference between them being that the distance between the walls in (b) is twice that of (a). From the results it is clear that in the smaller system (a), there is essentially no region where the density profile is even approximately flat. In (b), almost half the region between the walls has a flat density profile (it is easier to see it for the solvent because it has such regions in both compartments). It is also clear that after the adsorption layer, the densities are essentially constant in these systems, and that for the solvent the density of the adsorbed layer is higher on the solution side, compared to that in the solvent compartment. Figure 6(c) corresponds to a system identical to (b), but with  $N_S = 112$ , i.e., the overall solvent density is lower. Comparing (b) and (c), it can be seen that at lower densities the (relative) adsorption effects are roughly 10 per cent higher. In addition the regions of constant (flat) density profiles are more pronounced. Figure 6(d) corresponds to a system similar to 6(c) but with a much higher solute concentration ( $N_B = 100$ ). At these higher concentrations, the adsorption effects appear to be relatively weaker. Although the overall solute density in the solutions compartment is higher in (d) compared to that in (c), by a factor of 5, the density of the adsorbed layer is higher by a factor of 3. For the solvent, the average solvent density has decreased by approximately 25 per cent, but the density of the adsorbed layer is down by 35 per cent. This drop is somewhat compensated for, on the solution side by a weak second peak in the density profile of both the solute and solvent, adjacent to the adsorbed layer. Finally, the density profiles in the  $y$  and  $z$  direction are almost constant with weak oscillations (about 10 per cent of the average density values) centered at the sites of the wall molecules in the  $yz$  plane (not shown in Fig. 6).

The osmotic pressure for simulations of cubic systems ( $L = 7$ ) measured as described in the previous section, is reported in Fig. 7. It is clear that at low

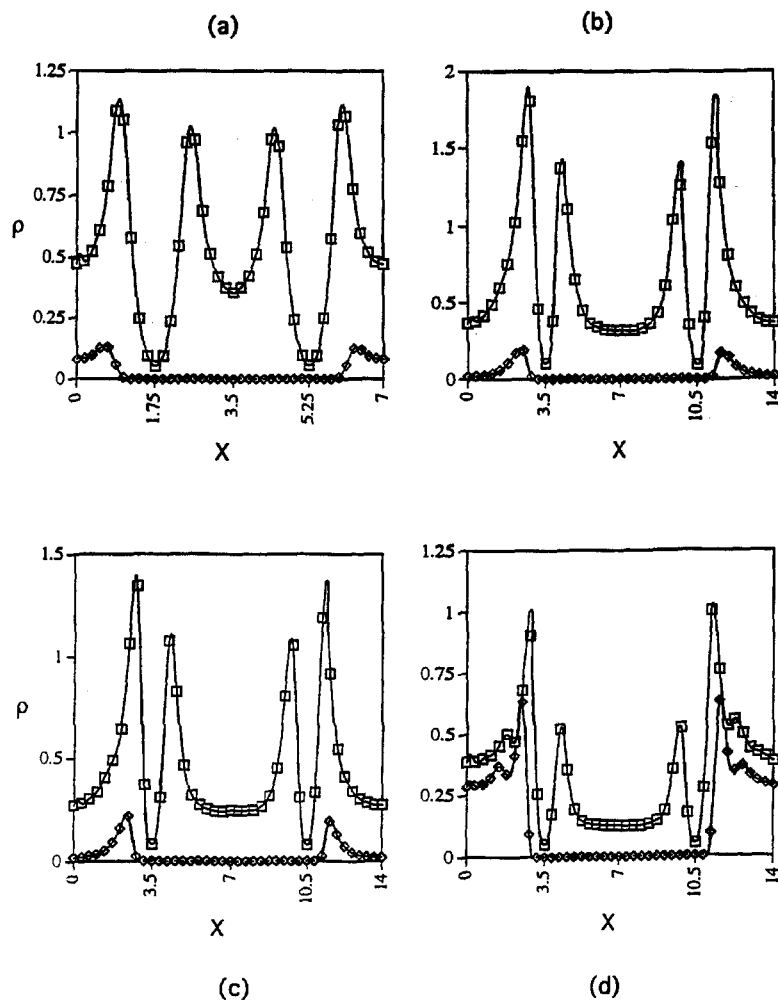


Figure 6. Density profiles of the solvent and solute molecules for a range of system variables (see text). (□) solvent, (◇) solute.

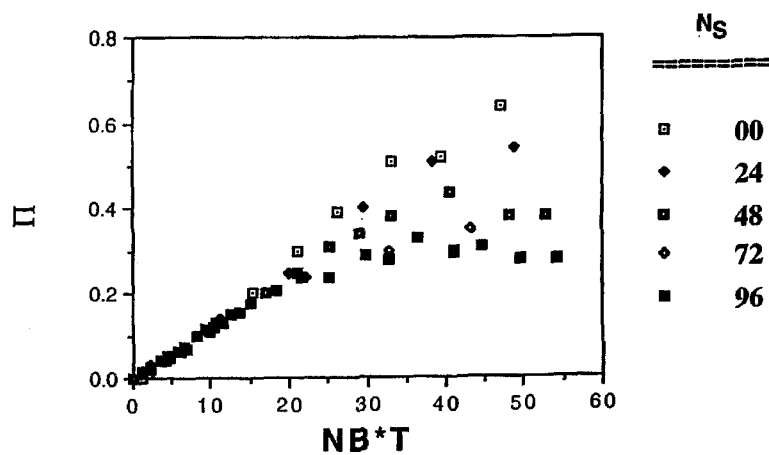


Figure 7. The osmotic pressure ( $\Pi$ ) for the cubic system as a function of solvent concentration, at different initial densities of the solvent ( $N_S$ ).

concentrations, the osmotic pressure varies linearly with  $N_B$  ( $T$  was essentially kept fixed in these simulations). Such a linear dependence is also suggested by van't Hoff's equation (Taylor, 1925; Weissberger, 1960) which also requires that the slope of this line be equal to the reciprocal of the volume of the solution compartment. However, van't Hoff's equation requires homogeneous density profiles in both the solution and solvent compartments (or at least a significant fraction thereof) as well as dilute solutions. As is clear from Fig. 6, which gives the solvent and solute density profiles in the solvent and solution compartments, this is not even approximately correct in our simulations even in the larger system studied. It is therefore possible that at other state conditions and/or different solvent/solute parameters we may not get a linear relationship between  $\Pi$  and  $N_B$  over as wide a range of concentrations as shown in Fig. 7. To obtain accurate estimates of the osmotic pressure rather long simulations must be carried out. This is necessary because one must measure small pressure differences between the two compartments, and pressures are notoriously difficult to measure in the first instant. Consequently we only report results for the smaller system ( $L = 7$ ). For the larger system ( $L_x = 2L_y = 2L_z = 14$ ), we were unable to carry such long simulations, but we expect the results to be similar to those shown in Fig. 7. We would like to point out that we have carried out some simulations using Gibbs Ensemble Monte-Carlo for similar systems (Panagiotopoulos et al., 1988), in which by the nature of the algorithm, both the compartments are homogeneous. We have found out that in such homogeneous systems the concentration region in which van't Hoff equation applies almost doubles (upto  $N_B = 60$ ).

#### 4. Conclusions

We have presented computer simulation studies of osmosis and reverse osmosis in solutions. The method developed should prove useful in examining reverse osmosis for a large range of solutions, including the more interesting aqueous solutions, that we plan to report in a future communication.

#### Nomenclature

- $D_{\perp}$  Diffusion coefficient perpendicular to the semi permeable wall  
 $D_{\parallel}$  Diffusion coefficient parallel to the semi permeable wall

- $L$  Size of the simulation cube  
 $L_{\alpha}$  Length of the simulation system in the  $\alpha$  direction ( $\alpha = x, y, z$ )  
 $N_B$  Number of solute molecules in the solution compartment  
 $N_C$  Net number of solvent molecules that move from the solvent compartment to the solution compartment during the simulation  
 $N_S$  Number of solvent molecules initially in the solvent compartment  
 $T$  Temperature of the system  
 $\epsilon$  Lennard-Jones energy parameter  
 $\rho$  Density  
 $\sigma$  Lennard Jones size parameter

#### Acknowledgments

This research was supported by grants from the US Department of Energy (grant no. FG02-87ER-13769), and the Petroleum Research Fund administered by the American Chemical Society. Travel funds were provided by the National Science Foundation (INT-9123242).

#### References

- Banavar, J.R., J. Koplik, and J.F. Willemsen, *Computer Simulation Studies in Condensed Matter Physics III*, Vol. 53, Springer Proceedings in Physics, Springer-Verlag, Berlin, 1990.  
 Bojan, M.J., A.V. Vernov, and W.A. Steele, "Simulation Studies of Adsorption in Rough Walled Cylindrical Pores," *Langmuir*, **8**, 901 (1992).  
 van't Hoff, J.H., "Die Rolle des Osmotischen Drucken in der Analogie Zwischen Losungen und Gasen," *Z. Phys. Chem.*, **1**, 481 (1887).  
 Hoornaert, P., *Reverse Osmosis*, Pergamon, Oxford, 1984.  
 Mo, G. and F. Rosenberger, "Molecular Dynamics Simulation of Flow in a Two Dimensional Channel with Atomically Rough Walls," *Phys. Rev. A*, **42**, 4688 (1990).  
 Murad, S., P. Ravi, and J.G. Powles, "A Computer Simulation Study of Fluids in Slit, Tubular, and Cubic Micropores," *J. Chem. Phys.*, **98**, 9771 (1993).  
 Murad, S., P. Ravi, and J.G. Powles, "Anisotropic Thermal Conductivity of a Fluid in a System of Microscopic Slit Pores," *Phys. Rev. E*, **48**, 4110 (1993a).  
 Panagiotopoulos, A.Z., N. Quirke, M. Stapleton, and D.J. Tildesley, "Phase Equilibria by Simulation in the Gibbs Ensemble-Alternative Derivation, Generalization, and Application to Mixtures and Membrane Equilibria," *Mol. Phys.*, **63**, 527 (1988).  
 Sourirajan, S., *Reverse Osmosis*, Academic, New York, 1970.  
 Taylor, H.S., *A Treatise on Physical Chemistry*, Van Nostrand, New York, 1925.  
 Weissberger, A. (Ed.), *Physical Methods of Organic Chemistry*, Part 1, Chapter 6, Interscience, New York, 1960.